2023 IEEE Symposium Series on Computational Intelligence (SSCI)
Mexico City, Mexico. December 5-8, 2023

A Comparative Study of Pretrained Deep Neural Networks for Classifying Alzheimer's and Parkinson's Disease

Vimbi Viswan
College of Computing and Inf.Sc
UTAS
Sohar, Oman
vimbi.viswan@utas.edu.om

Noushath Shaffi
College of Computing & Inf.Sc
UTAS
Sohar, Oman
noushath.shaffi@utas.edu.om

Mufti Mahmud
Department of Computer Science
Nottingham Trent University
Nottingham, United Kingdom
mufti.mahmud@ntu.ac.uk

Karthikeyan Subramanian
College of Computing & Inf.Sc
UTAS
Sohar, Oman
karthikeyan.supramanian@utas.edu.om

Faizal Hajamohideen
College of Computing & Inf.Sc
UTAS
Sohar, Oman
faizal.hajamohideen@utas.edu.om

***Abstract*—Early detection of neurodegenerative diseases can be challenging, where Deep Learning (DL) techniques have shown promise. Most DL techniques provide a robust and accurate classification performance. However, due to the complex architectures of the DL models, the classification results are difficult to interpret, causing challenges for their adoption in the healthcare industry. To facilitate this, the current work proposes an effective and interpretable analysis pipeline that compares the performances of pre-trained models for the early detection of Alzheimer's Disease (AD) and Parkinson's Disease (PD). The proposed pipeline allows tuning of hyperparameters, such as batch size, number of epochs, and learning rates, to achieve more robust and accurate classification. Additionally, validation of predictions using heatmaps drawn from GradCAM are also provided.**

***Index Terms*—Deep Learning, Neurodegeneration, Alzheimer's Disease, Parkinson's Disease, Explainability, GradCAM.**

I. Introduction

Alzheimer's disease (AD) is a neurological disorder that affects the brain and causes a gradual decline in cognitive abilities, memory, and daily activities [1]. It is progressive and irreversible, worsening over time and significantly impacting a person's quality of life. AD is characterised by abnormal protein deposits and tangled fibres in the brain, known as amyloid plaques and neurofibrillary tangles, respectively. Symptoms include memory loss, disorientation, difficulty with problem-solving and planning, language problems, and changes in mood and behaviour [2]. Parkinson's disease (PD) is a progressive neurological disorder that mainly impacts movement and motor control [3]. It arises due to the loss of dopamine-producing brain cells in the Substantia Nigra, a brain region responsible for transmitting movement signals. As these cells degenerate, individuals experience various motor symptoms that gradually worsen over time. These symptoms include tremors, bradykinesia (slow movement), muscle rigidity, and postural instability [4] (see Figure 1).

AD and PD are major neurological conditions that have a significant impact on global health and mortality rates. AD is the most common cause of dementia and affects many people worldwide, particularly older individuals. According to the World Alzheimer's Report 2022, there are currently 55 million people living with AD worldwide, which is predicted to reach 78 million by 2030 [5]. PD doesn't usually directly cause death. However, it can lead to severe complications that can contribute to mortality. For example, falls caused by motor symptoms, difficulty swallowing leading to aspiration pneumonia, and other related issues can increase the risk of death in individuals with PD. The latest global estimates show that PD led to 5.8 million disability-adjusted life years and resulted in approximately 329,000 deaths [3].

As AD advances, the patients may lose their ability to carry out daily activities like bathing, dressing, or cooking, making them feel inadequate and dependent on others leading to frustration, confusion, and helplessness [6]. As the disease progresses, AD patients may lose their sense of self and identity as their memories, skills, and abilities gradually deteriorate. In the final stages of AD, patients may need specialized end-of-life care, which can pose additional challenges for families and caregivers [7]. PD is primarily characterised by motor symptoms such as tremors, muscle rigidity, slow movement, and difficulty with balance. These symptoms can make everyday tasks challenging, leading to frustration and loss of

This work is funded by the Ministry of Higher Education, Research and Innovation (MoHERI) of the Sultanate of Oman under the Block Funding Program (Grant number: MoHERI/BFP/UoTAS/01/2021). Mufti Mahmud is supported by the NTU CIRC-QR Fund 2023-2024 and the British Embassy in Kuwait through the project titled 'Investigation of Emotional Deficits in Parkinson's Disease using Advanced Machine Learning Methods.'

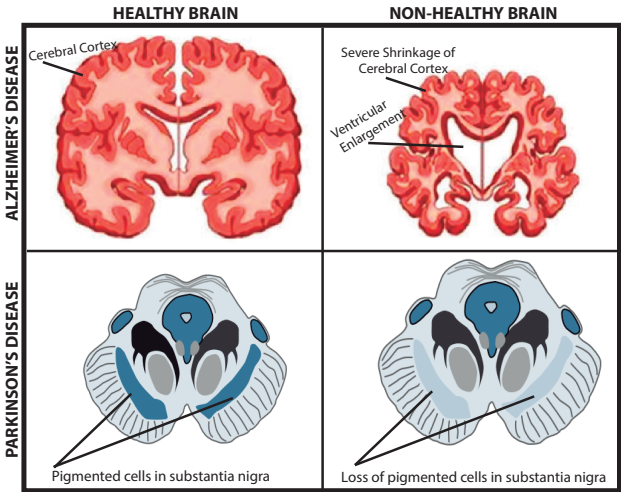

Fig. 1. Healthy and Non-healthy brain structure for Alzheimer's (Top) and Parkinson (Bottom) diseases.

independence. PD can also cause non-motor symptoms such as cognitive changes, depression, anxiety, sleep disturbances, and gastrointestinal problems. These symptoms can significantly impact patients' overall well-being and quality of life. As PD progresses, patients may experience emotional challenges with speech and communication, including mood swings, depression, anxiety, significant fatigue, and sleep disruption, leading to helplessness and loss of autonomy. AD and PD inflict significant suffering on patients and their families. These chronic and progressive conditions lack a cure, but early detection and treatment can help manage symptoms, slow disease progression, and improve patients' quality of life. Detecting and diagnosing neurodegenerative disorders like AD and PD can be significantly aided by AI tools [8].

AI and medical research continuously evolve, and newer models may have emerged. For instance, convolutional neural networks (CNN) architectures, like ResNet50, ResNet101, ResNet152, InceptionV3, IncveptionResNetV2, and EfficientNetB0 have been employed in medical image analysis tasks, including AD and PD detection [9], [10]. Interesting effectiveness in image classification tasks using InceptionV3 has been observed. It is a strong candidate for medical image analysis due to its efficient feature extraction, deep architecture allowing learning of hierarchical data representations, and reduced use of parameters.

There is a vast amount of literature on the detection and management [11], [12] and modelling [13] of neurodegenerative diseases from neuroimages [2], [6], [7], [14]–[18], brain signals [19]–[21], wearables [22]–[24], and clinical data [25]–[27]. Many of the classification methods used for AD and PD heavily relied on feature transfer learning (TL) and CNN [28]. Ghazal et al. [29] introduced a new technique that can be used to classify brain images obtained through MRI scans into four categories for AD. Meanwhile, [30] conducted a study that employed pre-trained weights from established datasets and retrained the fully connected layer using only a small number of MRI images. The results showed that this approach could generate comparable or even better outcomes than current deep-learning-based methods, despite using a training dataset that is almost ten times smaller than popular ones. Additionally, Aderghal et al. [31] investigated the use of diffusion tensor imaging together with structural MRI to study AD. By using this approach, overfitting is reduced and learning performance is improved, resulting in more accurate predictions.

Mehmood et al. [32] proposed a technique for detecting AD at an early stage using MRI images and TL. They employed a pre-trained CNN model and fine-tuned it to a smaller dataset of MRI images, achieving an accuracy rate of more than 80% on the test dataset. Similarly, in [33], the authors suggest combining CNN and recurrent neural networks (RNN) to analyze sequences of images for each subject. The authors found that the features extracted from CNN when trained with RNN, have significantly enhanced the system's accuracy.

A study conducted by James et al. [34] suggests that deep learning (DL) can be used to diagnose Parkinson's Disease (PD) using MRI and dopamine transporter scans. Their approach involves analyzing and utilizing the knowledge obtained by deep CNN and recurrent neural networks (RNN). Another recent study [35] used various factors such as Rapid Eye Movement, olfactory loss, and data on Cerebrospinal fluid and dopaminergic imaging markers to create a deep learning model. This model achieved an impressive average accuracy rate of 96.45%, surpassing twelve other machine learning and ensemble learning techniques.

Explainable AI (XAI) is a set of features that interprets the predictions from ML/DL models to get humans to trust and use the system efficiently. We suggest referring to the cited article for a comprehensive understanding of the concepts of interpretability or XAI [17]. Despite the vast literature, the interpretation and explainability of models' workability lack transparency, making their adoption difficult [36]. Additionally, the affinity between the original input image and the interpretation of predictions must be adequately discussed.

To address the aforementioned limitations, we propose a thorough process for classifying AD/PD using pre-trained DL models, namely, ResNet50, ResNet101, ResNet152, InceptionV3, InsceptionResNetV2, and EfficientNetB0. Additionally, the XAI tool, GradCAM, is used to validate the results. GradCAM provides visual explanations or heatmaps by highlighting the region of input images contributing most to the model's prediction [37]. We also used Pearson's correlation factor, which is a metric used to assess the measure of correlation between the effectiveness of the heatmap in capturing the features of an MRI image. It helps in highlighting the relevant regions of interest for predicting the class accurately.

The paper is structured as follows: Section II describes the proposed methodology, section III presents the results and their analysis, while section IV concludes the paper.

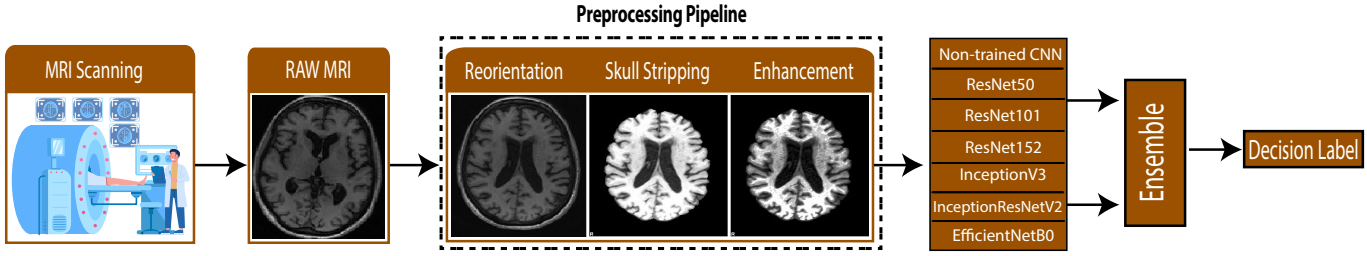

Fig. 2. A diagram depicting the proposed methodology.

II. Proposed Methodology

This study classifies AD and PD using pre-trained DL models, such as ResNet50, ResNet101, ResNet152, InceptionV3, InceptionResNetV2, and EfficientNetB0. The proposed methodology comprises three key components as shown in Fig. 2: 1) fine-tuning pre-trained models, 2) testing and prediction with axial plane images, and 3) interpreting predictions. The aim of the experiment was to compare the performance of these models and determine the most effective one. Initially, we fine-tuned the pre-trained models for AD by removing the top layer, keeping the rest of the network frozen, and retaining the ImageNet weights. In the next step, we obtained the last convolutional layer output and predictions for the axial plane. Finally, we interpreted the final axial plane results from the last convolutional layer using the GradCAM technique [37]. Pearson's correlation coefficient [38] was used to measure the affinity between the heatmap and the original MRI image.

A. Fine-Tuning Pre-trained Deep Neural Networks

The AD detection experiments using pre-trained models employed transfer learning by removing the top layer while keeping the rest of the network frozen with retained ImageNet weights. The fine-tuning layer can be denoted as $DO(0.5) - Flatten - BN - 2048N - BN - DO(0.5) - 1024N - BN - DO(0.5) - 4N$, where $DO(x)$ represents a dropout layer with a dropout probability of x, BN stands for Batch Normalisation, and fN refers to a fully connected layer with f neurons. The final output layer consists of four neurons for the four AD classes and employs a softmax activation function. For PD, we applied the same fine-tuning layer as used for AD, except that the final output layer has two neurons and utilizes a softmax activation function.

The non-pre-trained CNN architecture for AD consisted of: $16C2 - 16C2 - MP2 - 32C2 - 32C2 - 32C2 - MP2 - 64C2 - 16C1 - Flatten - 4N$ layers. Here, nCk refers to the convolutional layer of n filters and $k \times k$ feature map, $MP2$ refers to the max-pooling layer, and kN refers to the output layer for k-way classification. A binary classification was performed for PD from the NTUA dataset using a CNN model as above except the output layer kN had neurons suitable for binary classification $(k = 2)$.

B. Magnetic Resonance Imaging and Preprocessing

This study used T1-weighted MRI data from two datasets: the Alzheimer's Disease Neuroimaging Initiative (ADNI) for AD and the National Technical University of Athens (NTUA) for PD. The ADNI dataset contained MRI scans from individuals aged 50-65 across four categories and the axial plane was used to obtain 1056 images– AD: 223, early mild cognitive impairment (EMCI): 475, late mild cognitive impairment (LMCI): 262, and cognitively normal (CN): 96. The dataset was split into a 90:10 for the test:train ratio (950:106). The NTUA dataset included binary labels based on the severity of the disorder which were measured by the Clinical Dementia Rating (CDR) score. A CDR score of 0.0 indicated no dementia, while a score of 1.0 indicated PD. There were 1284 and 1422 images in the CDR-0 and CDR1.0 categories, respectively. The images had a dimension of 128×128 and were split into a 70:30 train-test ratio.

The FMRIB Software Library toolset [9] was used in preparing the raw MRI scans from ADNI. The preprocessing consisted of four main steps: reorientation, registration, skull-stripping, and histogram equalisation. These preprocessed images were then inputted to the proposed pipeline by transforming them to three-dimensional (3D) images.

C. Interpreting Results with GradCAM

The pre-trained models were fine-tuned to predict the MRI images from the axial plane only. To achieve this, a low learning rate of 0.0001, Adam activation, and a batch size of 128 were used. The number of epochs was determined using EarlyStopping (see Table I). The evaluation of the DL models was based on three performance metrics: Accuracy, Sensitivity, and Specificity [7]. We used Specificity to calculate the false-positive rate (FPR) as 1-Specificity, and we used Sensitivity to calculate the false-negative rate (FNR) as 1-Sensitivity.

To analyse the axial plane results of the last convolutional layer, we use the GradCAM technique [37]. By utilising

TABLE I
Hyperparameters used in the study

Hyperparamter	Value
Learning rate	0.0001
Activation Function	Adam
Epochs	200
Callbacks	EarlyStopping, ModelCheckpoint, ReduceLROnPlateau

TABLE II
RESULTS OF DL ALGORITHMS ON ADNI DATASET

Method	Test Acc	Train Acc	Val Acc	Specificity	Sensitivity	FNR	FPR	AUC
ResNet50	0.9890	0.9950	0.9989	0.9926	0.9803	0.0197	0.0074	0.9864
ResNet101	0.9620	0.9910	0.9911	0.9863	0.9695	0.0305	0.0137	0.9922
ResNet152	0.9809	0.9920	0.9924	0.9926	0.9803	0.0197	0.0074	0.9899
InceptionV3	0.9050	0.9990	0.9850	0.9682	0.9215	0.0785	0.0318	0.9912
InceptionResNetV2	0.9620	0.9980	0.9960	0.9841	0.9398	0.0602	0.0159	0.9917
EfficientNetB0	0.4380	0.6830	0.6907	0.7500	0.2500	0.7500	0.2500	0.5468

TABLE III
RESULTS OF DL ALGORITHMS ON NTUA DATASET

Method	Test Acc	Train Acc	Val Acc	Specificity	Sensitivity	FNR	FPR	AUC
ResNet50	0.9982	0.9999	0.9999	0.9961	1.0000	0.0000	0.0039	0.9999
ResNet101	0.9963	0.9999	0.9999	0.9961	0.9965	0.0035	0.0039	0.9999
ResNet152	0.9993	0.9999	0.9999	0.9992	0.9993	0.0007	0.0008	0.9999
InceptionV3	0.9804	0.9991	0.9981	0.9860	0.9754	0.0246	0.0140	0.9982
InceptionResNetV2	0.7868	0.8484	0.8852	0.6737	0.8888	0.1111	0.3263	0.8872
EfficientNetB0	0.9981	0.9979	0.9999	1.0000	0.9965	0.0035	0.0000	0.9999

gradient information from the final CNN layer, we generate a heatmap that highlights crucial image regions and provides explanations for predictions. This heatmap is then layered over the input image, which helps explain the influential regions. In the equation, $L^c_{GradCAM} = ReLU\left(\sum_k \alpha^c_k \cdot A^k\right)$, $L^c_{GradCAM}$ represents the GradCAM heatmap, α^c_k denotes the weights calculated for each feature map A^k, and the summation aggregates the weighted feature maps for a target class c. To ensure the heatmap only has positive values, the ReLU function is used. The GradCAM technique can be summarized by this equation, which helps identify the important regions in the input image that contribute to the predicted class.

$$\hat{X} = \frac{X - \mu_X}{\sigma_X} \tag{1}$$

$$\hat{Y} = \frac{Y - \mu_Y}{\sigma_Y} \tag{2}$$

$$cov = \frac{\sum_{i=1}^{n}\left((\hat{X} - \bar{X})(\hat{Y} - \bar{Y})\right)}{n-1} \tag{3}$$

$$\sigma_X = \sqrt{\frac{\sum_{i=1}^{n}\left(\hat{X}_i - \bar{X}\right)^2}{n-1}} \tag{4}$$

$$\sigma_Y = \sqrt{\frac{\sum_{i=1}^{n}\left(\hat{Y}_i - \bar{Y}\right)^2}{n-1}} \tag{5}$$

$$P_r = \frac{cov}{\sigma_X \cdot \sigma_Y} \tag{6}$$

Finally, we used the Pearson's coefficient [38] to correlate the heatmap with the original MRI image. The images were resized and converted into 1D vectors represented by X and Y and normalized using equations 1 and 2 where μ_X and μ_Y is the mean and σ_X and σ_Y is the standard deviation. The covariance of the normalized images is calculated using the equation 3 where n is the number of elements in the vector and $\bar{X}$ and $\bar{Y}$ are the means of X and Y, respectively. The standard deviations σ_X and σ_Y of the normalized vectors $\hat{X}$ and $\hat{Y}$ are computed as shown in equations 4 and 5. To determine the Pearson coefficient, we use Equation-6, and this value can range between -1 and +1. If the value is negative, it suggests a negative correlation. If the value is zero, it shows no correlation. If the value is positive, it indicates a positive correlation. The results and analysis section discusses the results obtained from Pearson's correlation analysis.

III. RESULTS AND DISCUSSION

In this section, we tabulated the performances of pre-trained neural network models from the ImageNet challenge (ResNet50, ResNet101, ResNet152, InceptionV3, Inception-ResNetV2, and EfficientNetB0) for AD from the ADNI dataset (Table II). Performance results from the selected neural network models are also tabulated for PD patients from the NTUA dataset (Table III). Table II shows that some models have outperformed others. Specifically, for the ADNI dataset, the ResNet50, ResNet101, InceptionV3, and InceptionResNetV2 models achieved AUC scores exceeding 0.98. In the case of the NTUA dataset, which dealt with binary classification for PD patients, Table III indicates that many models obtained AUC scores of over 0.99.

Figure 3 shows the confusion matrices for the four most effective algorithms in detecting AD from the ADNI dataset. The InveptionV3 model was able to distinguish between MCI and AD patients in the ADNI dataset with an accuracy of 95.6% and 81.5%, respectively. In the NTUA dataset, the confusion matrix for PD patients can be seen in Fig. 4. The ResNet50 model differentiated between non-PD and PD patients with 99.6% and 100% accuracy, respectively. Interpreting predic-

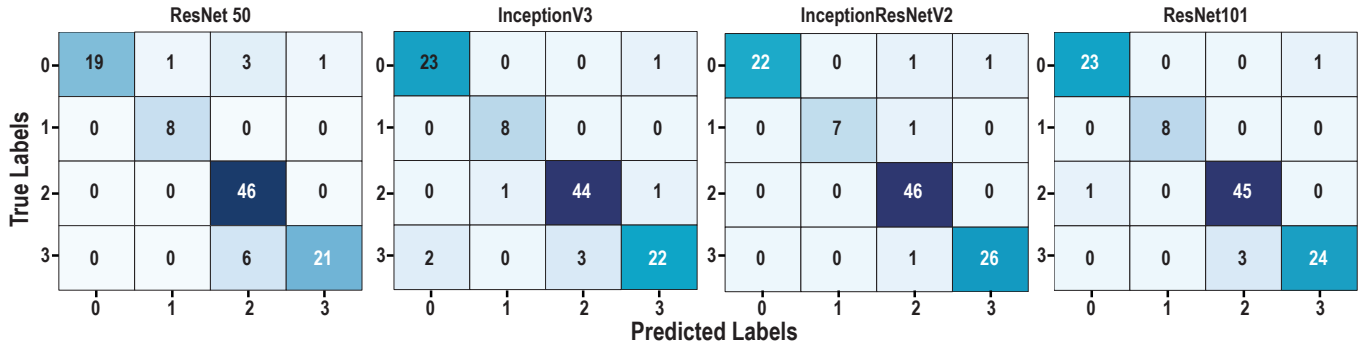

Fig. 3. Confusion matrices for 4 pretrained models for the ADNI dataset.

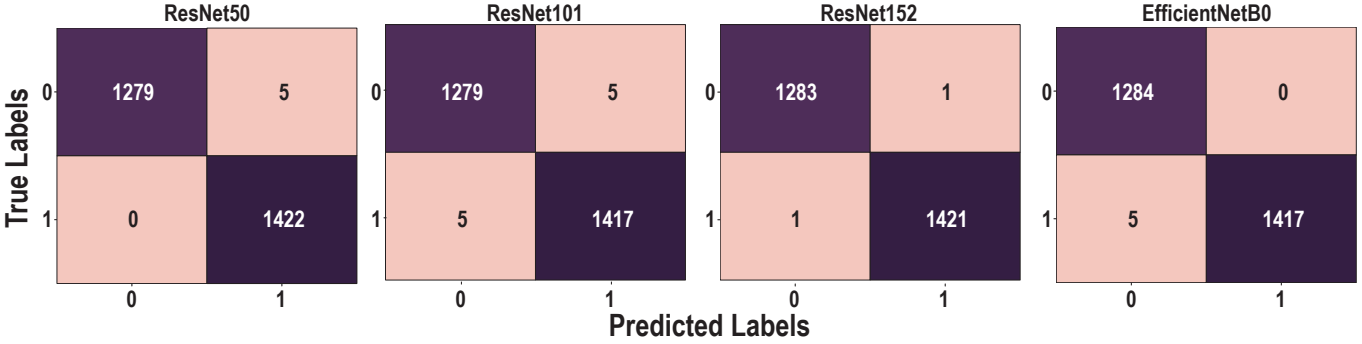

Fig. 4. Confusion matrices for 4 pretrained models for the NTUA dataset.

tions will help to bridge the gap between trustworthiness and accuracy. Towards this goal, further interpretation of this model using GradCAM was performed using a non-pretrained architecture mentioned in Section II-A. Interpretation helps to distinguish between healthy and disease-inflicted patients and is crucial for early detection and intervention to delay or prevent the onset of the disease.

The results were explained by generating a heatmap using the predictions from the last convolutional layer of the non-pre-trained CNN model. Figure 5 shows the original MRI image, GradCAM heatmap, and class overlays (CN vs. AD) for the axial plane. The 'red' regions in the overlays indicate a strong connection to the predicted class. The axial plane displays areas related to neurodegeneration, atrophy, or abnormal metabolic activity in AD. By examining all the heatmaps, clinicians can gain insights into the impact of AD-related changes in the brain. For accurate results, the heatmaps produced should undergo validation either with the assistance of clinicians or through a ground truth heatmap.

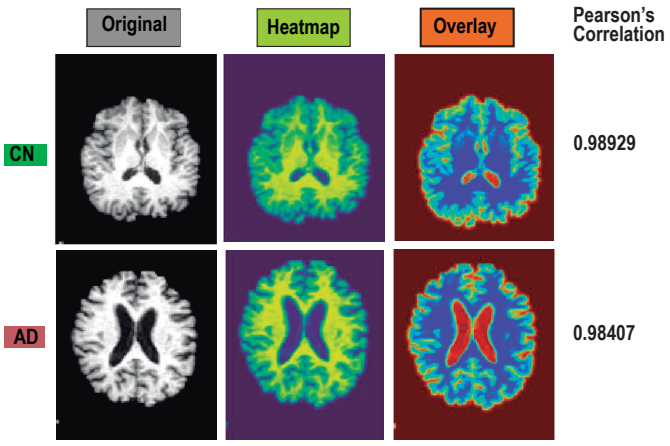

Fig. 5. Comparison between CN vs AD for original MRI image, heatmap, overlays, and Pearson's correlation coefficient for the axial plane.

In this experiment, we utilized Pearson's correlation coefficient to evaluate the correlation between the original MRI image and its heatmap. Our findings show that the axial plane demonstrated a strong positive correlation (refer to Figure 5). This positive correlation indicates that regions with higher intensity in the MRI image align closely with corresponding regions in the heatmap. As a result, higher positive correlations were observed for the predicted class. The Pearson correlation coefficient helps us determine how well the heatmap captures the MRI image's features, effectively highlighting relevant regions of interest for the predicted class.

IV. Conclusion

Our research involved analyzing six transfer learning algorithms using datasets from two neurological disorders, ADNI and NTUA. Our findings indicate that these algorithms can greatly enhance classification performance. However, we acknowledge that deep neural networks can be perceived as a "black box" due to their complex decision-making processes

[17]. We intend to investigate further and enhance the interpretability of these models to develop more precise and reliable automated diagnosis systems for neurodegenerative diseases.

REFERENCES

[1] T. C. Hammond, X. Xing, C. Wang, D. Ma, K. Nho, P. K. Crane, F. Elahi, D. A. Ziegler, G. Liang, Q. Cheng *et al.*, "β-amyloid and tau drive early alzheimer's disease decline while glucose hypometabolism drives late decline," *Commun. biol.*, vol. 3, 2020.

[2] N. Shaffi, V. Vimbi, M. Mahmud, K. Subramanian, and F. Hajamohideen, "Bagging the best: A hybrid svm-knn ensemble for accurate and early detection of alzheimer's and parkinson's diseases," in *Proc. Brain Inform.* Springer, 2023, pp. 443–455.

[3] W. H. Organization *et al.*, "Parkinson disease: a public health approach: technical brief," 2022.

[4] L. Sigcha, B. Domínguez, L. Borzì, N. Costa, S. Costa, P. Arezes, J. M. López, G. De Arcas, and I. Pavón, "Bradykinesia detection in parkinson's disease using smartwatches' inertial sensors and deep learning methods," *Electronics*, vol. 11, 2022.

[5] S. Gauthier, C. Webster, S. Sarvaes, J. Morais, and P. Rosa-Neto, "World Alzheimer Report 2022: Life after diagnosis - navigating treatment, care and support," 2022.

[6] F. Hajamohideen, N. Shaffi, M. Mahmud *et al.*, "Four-way classification of alzheimer's disease using deep siamese convolutional neural network with triplet-loss function," *Brain Inform.*, vol. 10, pp. 1–13, 2023.

[7] N. Shaffi, F. Hajamohideen, A. Abdesselam, M. Mahmud, and K. Subramanian, "Ensemble classifiers for a 4-way classification of alzheimer's disease," in *Proc. AII2022*, 2023, pp. 219–230.

[8] M. Mahmud, M. S. Kaiser, A. Hussain, and S. Vassanelli, "Applications of deep learning and reinforcement learning to biological data," *IEEE Transactions on Neural Networks and Learning Systems*, vol. 29, no. 6, pp. 2063–2079, 2018.

[9] M. B. T. Noor, N. Z. Zenia, M. S. Kaiser, S. A. Mamun, and M. Mahmud, "Application of deep learning in detecting neurological disorders from magnetic resonance images: a survey on the detection of alzheimer's disease, parkinson's disease and schizophrenia," *Brain Inform.*, vol. 7, pp. 1–21, 2020.

[10] M. Mahmud, M. S. Kaiser, T. M. McGinnity, and A. Hussain, "Deep learning in mining biological data," *Cogn. Comput.*, vol. 13, pp. 1–33, 2021.

[11] M. J. Al Nahian, T. Ghosh, M. N. Uddin, M. M. Islam, M. Mahmud, and M. S. Kaiser, "Towards artificial intelligence driven emotion aware fall monitoring framework suitable for elderly people with neurological disorder," in *Proc. Brain Inform.*, 2020, pp. 275–286.

[12] M. Nahiduzzaman, M. Tasnim, N. T. Newaz, M. S. Kaiser, and M. Mahmud, "Machine learning based early fall detection for elderly people with neurological disorder using multimodal data fusion," in *Proc. Brain Inform.*, 2020, pp. 204–214.

[13] D. Nagarajan, J. Kavikumar, M. Tom, M. Mahmud, and S. Broumi, "Modelling the progression of alzheimer's disease using neutrosophic hidden markov models," *Neutrosophic Sets Syst.*, vol. 56, no. 1, p. 4, 2023.

[14] M. B. T. Noor, N. Z. Zenia, M. S. Kaiser, M. Mahmud, and S. Al Mamun, "Detecting neurodegenerative disease from mri: a brief review on a deep learning perspective," in *Proc. Brain Inform.*, 2019, pp. 115–125.

[15] J. Ruiz, M. Mahmud, M. Modasshir, M. Shamim Kaiser, and f. t. Alzheimer's Disease Neuroimaging Initiative, "3d densenet ensemble in 4-way classification of alzheimer's disease," in *Proc. Brain Inform.* Springer, 2020, pp. 85–96.

[16] N. Shaffi, F. Hajamohideen, M. Mahmud *et al.*, "Triplet-loss based siamese convolutional neural network for 4-way classification of alzheimer's disease," in *Proc. BI2022*, 2022, pp. 277–287.

[17] V. Vimbi, N. Shaffi, M. Mahmud *et al.*, "Application of explainable artificial intelligence in alzheimer's disease classification: A systematic review," *Cogn. Comput*, pp. 1–36, 2023, [ePub Ahead of Print].

[18] S. Jahan, M. R. Saif Adib, M. Mahmud, and M. S. Kaiser, "Comparison between explainable ai algorithms for alzheimer's disease prediction using efficientnet models," in *Proc. Brain Inform.*, 2023, pp. 357–368.

[19] A. Leparulo, M. Mahmud, E. Scremin, T. Pozzan, S. Vassanelli, and C. Fasolato, "Dampened slow oscillation connectivity anticipates amyloid deposition in the ps2app mouse model of alzheimer's disease," *Cells*, vol. 9, no. 1, p. 54, 2019.

[20] M. A. Motin, M. Mahmud, and D. J. Brown, "Detecting parkinson's disease from electroencephalogram signals: An explainable machine learning approach," in *Proc. AICT2022*, 2022, pp. 1–6.

[21] M. Fabietti, M. Mahmud, A. Lotfi, A. Leparulo, R. Fontana, S. Vassanelli, and C. Fasolato, "Early detection of alzheimer's disease from cortical and hippocampal local field potentials using an ensembled machine learning model," *IEEE Trans. Neural Syst. Rehabil. Eng.*, vol. 31, 2023.

[22] T. M. Niamat Ullah Akhund, M. J. N. Mahi, A. Hasnat Tanvir, M. Mahmud, and M. S. Kaiser, "Adeptness: Alzheimer's disease patient management system using pervasive sensors-early prototype and preliminary results," in *Proc. Brain Inform.*, 2018, pp. 413–422.

[23] S. Jesmin, M. S. Kaiser, and M. Mahmud, "Artificial and internet of healthcare things based alzheimer care during covid 19," in *Proc. Brain Inform.* Springer, 2020, pp. 263–274.

[24] M. Biswas, A. Rahman, M. S. Kaiser, S. Al Mamun, K. S. Ebne Mizan, M. S. Islam, and M. Mahmud, "Indoor navigation support system for patients with neurodegenerative diseases," in *Proc. Brain Inform.*, 2021, pp. 411–422.

[25] Y. Miah, C. N. E. Prima, S. J. Seema, M. Mahmud, and M. Shamim Kaiser, "Performance comparison of machine learning techniques in identifying dementia from open access clinical datasets," in *Proc. ICACIn2020*, 2021, pp. 79–89.

[26] T. Chen, P. Su, Y. Shen, L. Chen, M. Mahmud, Y. Zhao, and G. Antoniou, "A dominant set-informed interpretable fuzzy system for automated diagnosis of dementia," *Front. Neurosci.*, vol. 16, p. 867664, 2022.

[27] T. Chen, C. Shang, P. Su, Y. Shen, M. Mahmud, R. Moodley, G. Antoniou, Q. Shen, and A. D. N. Initiative, "Assessing significance of cognitive assessments for diagnosing alzheimer's disease with fuzzy-rough feature selection," in *Proc. UK Workshop Comput. Intell.*, 2022, pp. 450–462.

[28] S. Shafiq, S. Ahmed, M. S. Kaiser, M. Mahmud, M. S. Hossain, and K. Andersson, "Comprehensive analysis of nature-inspired algorithms for parkinson's disease diagnosis," *IEEE Access*, vol. 11, pp. 1629–1653, 2022.

[29] T. M. Ghazal and G. Issa, "Alzheimer disease detection empowered with transfer learning," *Computers, Materials & Continua*, vol. 70, 2022.

[30] M. Hon and N. M. Khan, "Towards alzheimer's disease classification through transfer learning," in *2017 IEEE International conference on bioinformatics and biomedicine (BIBM)*. IEEE, 2017.

[31] K. Aderghal, A. Khvostikov, A. Krylov *et al.*, "Classification of alzheimer disease on imaging modalities with deep cnns using cross-modal transfer learning," in *Proc.CBMS*. IEEE, 2018, pp. 345–350.

[32] A. Mehmood, S. Yang, Z. Feng, M. Wang, A. S. Ahmad, R. Khan, M. Maqsood, and M. Yaqub, "A transfer learning approach for early diagnosis of alzheimer's disease on mri images," *Neuroscience*, vol. 460, 2021.

[33] A. Ebrahimi-Ghahnavieh, S. Luo, and R. Chiong, "Transfer learning for alzheimer's disease detection on mri images," in *Proc. IAICT*, 2019.

[34] J. Wingate, I. Kollia, L. Bidaut, and S. Kollias, "Unified deep learning approach for prediction of parkinson's disease," *IET Image Processing*, vol. 14, 2020.

[35] W. Wang, J. Lee, F. Harrou, and Y. Sun, "Early detection of parkinson's disease using deep learning and machine learning," *IEEE Access*, vol. 8, 2020.

[36] V. Hassija, V. Chamola, A. Mahapatra, A. Singal, D. Goel, K. Huang, S. Scardapane, I. Spinelli, M. Mahmud, and A. Hussain, "Interpreting black-box models: A review on explainable artificial intelligence," *Cogn. Comput.*, pp. 1–30, 2023.

[37] R. R. Selvaraju, M. Cogswell, A. Das, R. Vedantam, D. Parikh, and D. Batra, "Grad-cam: Visual explanations from deep networks via gradient-based localization," in *Proc. IEEE ICCV*, 2017, pp. 618–626.

[38] B. Turkbey *et al.*, "Correlation of magnetic resonance imaging tumor volume with histopathology," *J. Urol.*, vol. 188, 2012.